

Frequency-dependent magnetotransport phenomena in a hybrid Fe/SiO₂/p-Si structure

Cite as: J. Appl. Phys. **112**, 123906 (2012); <https://doi.org/10.1063/1.4769788>

Submitted: 06 September 2012 . Accepted: 16 November 2012 . Published Online: 18 December 2012

N. V. Volkov, A. S. Tarasov, E. V. Eremin, A. V. Eremin, S. N. Varnakov, and S. G. Ovchinnikov



View Online



Export Citation



CrossMark

ARTICLES YOU MAY BE INTERESTED IN

Extremely large magnetoresistance induced by optical irradiation in the Fe/SiO₂/p-Si hybrid structure with Schottky barrier

Journal of Applied Physics **114**, 093903 (2013); <https://doi.org/10.1063/1.4819975>

Magnetic-field- and bias-sensitive conductivity of a hybrid Fe/SiO₂/p-Si structure in planar geometry

Journal of Applied Physics **109**, 123924 (2011); <https://doi.org/10.1063/1.3600056>

Extremely high magnetic-field sensitivity of charge transport in the Mn/SiO₂/p-Si hybrid structure

AIP Advances **7**, 015206 (2017); <https://doi.org/10.1063/1.4974876>



Your Qubits. Measured.

Meet the next generation of quantum analyzers

- Readout for up to 64 qubits
- Operation at up to 8.5 GHz, mixer-calibration-free
- Signal optimization with minimal latency

Find out more



Frequency-dependent magnetotransport phenomena in a hybrid Fe/SiO₂/p-Si structure

N. V. Volkov,^{1,2,a)} A. S. Tarasov,¹ E. V. Eremin,^{1,2} A. V. Eremin,¹ S. N. Varnakov,^{1,2} and S. G. Ovchinnikov¹

¹*Kirensky Institute of Physics, Russian Academy of Sciences, Siberian Branch, Krasnoyarsk 660036, Russia*

²*Siberian State Aerospace University, Krasnoyarsk 660014, Russia*

(Received 6 September 2012; accepted 16 November 2012; published online 18 December 2012)

We report the large magnetoimpedance effect in a hybrid Fe/SiO₂/p-Si structure with the Schottky barrier. The pronounced effect of magnetic field on the real and imaginary parts of the impedance has been found at temperatures 25–100 K in two relatively narrow frequency ranges around 1 kHz and 100 MHz. The observed frequency-dependent magnetotransport effect is related to the presence of localized “magnetic” states near the SiO₂/p-Si interface. In these states, two different recharging processes with different relaxation times are implemented. One process is capture-emission of carriers that involves the interface levels and the valence band; the other is the electron tunneling between the ferromagnetic electrode and the interface states through SiO₂ potential barrier. In the first case, the applied magnetic field shifts energy levels of the surface states relative to the valence band, which changes recharging characteristic times. In the second case, the magnetic field governs the spin-dependent tunneling of carriers through the potential barrier. The “magnetic” interface states originate, most likely, from the formation of the centers that contain Fe ions, which can easily diffuse through the SiO₂ layer. © 2012 American Institute of Physics. [<http://dx.doi.org/10.1063/1.4769788>]

I. INTRODUCTION

Hybrid nanostructures combining nonmagnetic semiconductor and ferromagnetic elements have been the subject of intense study as promising candidates for spintronic applications.¹ The huge potential of modern semiconductor electronics intrinsic to these structures can be significantly enhanced by using, along with a charge, the spin degrees of freedom. However, application of hybrid structures requires clarifying some fundamental items, including injection and detection of the spin polarization,² control of spin transport in a semiconductor,³ spin accumulation,⁴ spin relaxation, etc.⁵

Of great interest are the dynamic characteristics of these structures, in particular, the alternating current (ac) electrical properties. Impedance and magnetoimpedance in magnetic nanostructures are important to investigate for application of the latter in high-frequency devices.^{6,7} On the other hand, the use of impedance spectroscopy allows one to elucidate the nature of the phenomena occurring in hybrid structures. For example, investigation of impedance and magnetoimpedance makes it possible to separate dynamic contributions of charge and spin transport and relaxation in different parts of inhomogeneous materials and nanostructures.⁸

The key question to be answered is how strong can be the effect of the spin state of carriers on the ac transport properties of hybrid structures and how effectively can the spin state of electrons and holes in these structures be controlled under the dynamic action of the electric and magnetic fields. Studies of magnetic tunnel junctions showed that

magnetic field can affect differently the direct current (dc) and ac transport.^{9–11} Magnetoimpedance in the tunneling structures can exceed by far the dc magnetoresistance. The value and sign of magnetoimpedance can change with bias voltage and frequency of the alternating current. The responses of the real and imaginary parts of impedance to magnetic field can be significantly different. Certainly, the ac magnetic transport is based on the spin-dependent tunneling of electrons through a potential barrier; however, the role of the structure interfaces and the processes of charge and spin accumulation on the interfaces is by far greater. In addition, it was shown that certain features in the behavior of magnetoimpedance can be attributed to the interplay of the spin and charge dynamics.

So far, the transport and magnetotransport properties of hybrid structures and spin injection and spin transport in them have been intensively studied only on a direct current.^{2,3,12} We failed to find any works on the ac impedance and magnetoimpedance. This fact motivated us to study impedance of the magnetic-semiconductor hybrid system as a function of a magnetic field.

Previously, we studied the dc transport and magnetotransport properties of the Fe/SiO₂/p-Si hybrid structure.¹³ It was shown that peculiarities of the transport properties are related to a metal-insulator-semiconductor (MIS) transition with the Schottky barrier near the interface between SiO₂ and p-Si. Resistance of the MIS transition depends on bias voltage and temperature, which determines the features of the temperature behavior of resistance and the dependence of the later on the current flowing through the structure. Also this structure exhibits the magnetoresistive effect; depending on temperature and bias, either positive or negative

^{a)}e-mail: volk@iph.krasn.ru.

magnetoresistance is observed. We attributed positive magnetoresistive effect to the processes occurring when the current flows into the semiconductor body. The negative effect is related, in our opinion, to the thin inversion layer that forms at the $\text{SiO}_2/\text{p-Si}$ interface. It is not improbable that certain role is played by the ferromagnetic state of the upper layer of the structure and by the spin-dependent tunneling of electrons across the $\text{SiO}_2/\text{p-Si}$ interface. In such a situation, the origin of the magnetoresistive effects can be clarified by the impedance spectroscopy. Here, we report frequency-dependent magnetoresistance and magnetoreactance of a $\text{Fe}/\text{SiO}_2/\text{p-Si}$ lateral device.

II. EXPERIMENTAL

A $\text{Fe}/\text{SiO}_2/\text{p-Si}$ structure was formed on a p-doped silicon wafer with a resistivity of $5 \Omega\text{-cm}$ (a doping density of $2 \times 10^{15} \text{cm}^{-3}$). The thicknesses of the SiO_2 and Fe layers were 1.2 and 5 nm, respectively. Preparation of the structure was described elsewhere.¹³ The sample to be studied represented a simple lateral device, commonly referred to as back-to-back Schottky diode. On the surface of the structure, two electrodes separated by $20\text{-}\mu\text{m}$ gap were formed from a continuous iron film. The schematic of the device is shown in the inset in Fig. 1(a), and the sample size is 3 by 8mm^2 . The desired topology of the electrodes was formed with a coordinatograph of the original design by wet etching. Ohmic contacts were formed on the top of Fe electrodes with the use of two-component silver epoxy.

To study impedance spectra of the sample, we used the two-probe setup. Measurements in the frequency range from 20Hz to 1GHz were performed with Agilent E4980A and Agilent 4287A impedance analyzers. During our measurements, the oscillating voltage was fixed at 10mV and dc magnetic field up to 10kOe was generated by electromagnet oriented either parallel or perpendicular to the plane of the structure. The measurements were performed in the helium cryostat with the temperature accuracy better than 0.1K .

III. RESULTS AND DISCUSSION

A. Impedance without magnetic field

The frequency-dependent magnetotransport phenomena in the device (back-to-back Schottky diode) formed from the hybrid $\text{Fe}/\text{SiO}_2/\text{p-Si}$ structure were investigated in detail by measuring the real (R) and imaginary (X) parts of the impedance $Z = R + iX$. The experimental impedance data can be analyzed using theoretical model that describes the actual charge transport processes in the structure. The other way is to analyze an empirically selected electrical equivalent circuit of the device and then attempt to relate actual physical parameters and processes to the elements of this circuit. Below we use mainly the first approach as more physically grounded.

Before we proceed to the discussion of the magneto-dependent effects, consider the behavior of the structure in zero magnetic field. Temperature dependence of R and X at different frequencies in zero magnetic field is shown in Fig. 1. It can be clearly seen that the real part of the impedance has

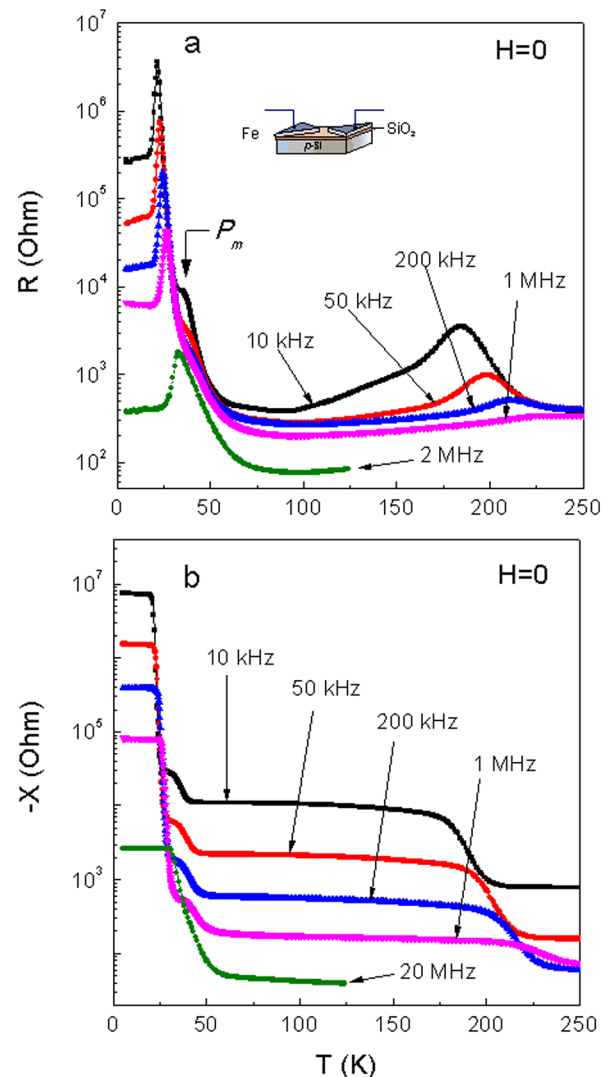


FIG. 1. Temperature dependences of (a) the real and (b) imaginary parts of the impedance at different frequencies for the back-to-back $\text{Fe}/\text{SiO}_2/\text{p-Si}$ diode device in zero magnetic field. P_m designates the “magnetosensitive peak.” Inset: schematic of the device and the measurement setup.

three peaks. Their positions and heights depend on frequency. The broad peak at high temperatures is the most frequency-dependent: as the frequency is increased, it strongly shifts towards higher temperatures and its intensity rapidly drops. The same trend is characteristic to the narrow intense peak in the low-temperature ($20\text{--}30 \text{K}$) region, although its shift along the temperature axis with varying frequency is not that pronounced. We should emphasize the feature (peak) of R at temperatures of $30\text{--}40 \text{K}$. As we will see later on, it is this peak that determines the sensitivity of the structure to magnetic field. Hereinafter, this peak is referred to as magnetosensitive and designated in the figures as P_m . Unfortunately, localization of the magnetosensitive peak on the slope of the much more intensive peak does not allow us to completely resolve it. While at low frequencies of the alternating signal, the P_m peak can be clearly seen; with increasing the frequency, its intensity rapidly drops and the peak smears and is almost completely absorbed by the intense low-temperature peak on the $R(T)$ dependence.

Concerning the imaginary part of the impedance, it is negative, i.e., the main contribution to the latter is capacitive ($X = X_L - X_C, X_L \ll X_C$). In addition, in the temperature dependence of X , there are steps that correspond to the peaks in the temperature dependence of R . It is noteworthy that the above-mentioned feature of R near 30–40 K, which is poorly resolved at low frequencies, becomes pronounced in the $X(T)$ dependence up to 10 MHz.

Generally speaking, the presence of the peaks and steps in the temperature dependences of the real and imaginary parts of impedance is no surprise if all the features of the transport properties of the structure under study are attributed to the presence of the MIS transition with Schottky barrier near the interface between SiO_2 and p-Si (Fig. 2(a)).¹³ Indeed, these features are observed in actual MIS structures¹⁴ and caused by recharging of the surface states and impurity centers localized near the oxide-semiconductor interface. Since we are interested merely in the centers localized within the Schottky barrier, for clarity hereinafter they are referred to just as surface centers.

The shift in the MIS structure bends edges of energy bands on the dielectric-semiconductor interface. Since in this case, the levels of the surface centers retain their position relative to the boundaries of the valence and conduction bands, the shift leads to the variation in the energy gap between the Fermi level and the energy levels of the surface centers. When small ac voltage is applied to the MIS structure, the Fermi level sweeps through different defect energy levels and induces recharging of the interface centers. If the energy levels of the center appear above the Fermi level, the center tends to ionize; if the situation is opposite, it tends to capture a charge. This process of recharging of the surface states with varying voltage on the MIS structure is inertial, to a certain extent. The rate of this process is limited by either the rate of capture of carriers on the surface levels or the rate of injection of carriers to the allowed bands of a semiconductor. Thus, R and X reveal the features each time when the condition $\omega\langle\tau\rangle = 1$ is met, where $\langle\tau\rangle$ is the average constant of the time of recharging of the centers and $\omega = 2\pi f$ is the angular frequency of the applied ac signal. The temperature dependences can be analyzed as follows. As the temperature is decreased, the Fermi level in the p-type semiconductor low-

ers approaching the boundary of the valence band; at certain temperatures, the Fermi level and the interface levels cross. At this moment, the charge of the centers changes the most and if at fixed frequency ω the condition $\omega\langle\tau\rangle = 1$ is met, then there is the peak in the temperature dependence of the real part of the impedance and the corresponding step on the temperature dependence of the imaginary part.¹⁵ The frequency dependence of the position and height of the peak is determined by the temperature dependence of $\langle\tau\rangle$ and the distribution of the density of surface states in the forbidden gap of semiconductor.

The relaxation time of the surface states can be interpreted also as the time constant of charging the differential capacitance of the surface states. The equivalent circuit of the MIS structure with regard to the surface states is shown in Fig. 2(b). For the equivalent circuit of the ideal MIS structure, i.e., regardless of electrons tunneling through the dielectric layer, the relaxation time is $\langle\tau\rangle = C_S R_S$, where C_S and R_S are the equivalent capacitance and resistance that take into account recharging of the surface states. Tunneling, which is clear characteristic of thin dielectric layer (as in our case) can be considered as one more channel of recharging of the centers in addition to the recharging mechanisms in which the allowed bands of the semiconductor participate. Within the equivalent circuit, tunneling through the potential barrier can be taken into account by introducing equivalent resistances R_T and R_{ST} (Fig. 2(b)) that characterize tunneling of electrons to the valence band and the surface states, respectively.

Obviously, the presence of the characteristic times of recharging of the surface centers should manifest itself also in the frequency dependences. The frequency dependences of R and X are presented in Fig. 3. The dependences are given for the temperature range 30–100 K, since, as we show below, these temperatures correspond to the most significant change in the impedance in a magnetic field. For all the temperatures, starting from the lowest frequencies, $R(f)$ and $X(f)$ decrease monotonically with increasing frequency. In the high-frequency region, however, the features are observed typical of systems with the Debye relaxation processes. One of these features, the steps in the $R(f)$ dependence and the corresponding peaks in the $X(f)$ dependence, is

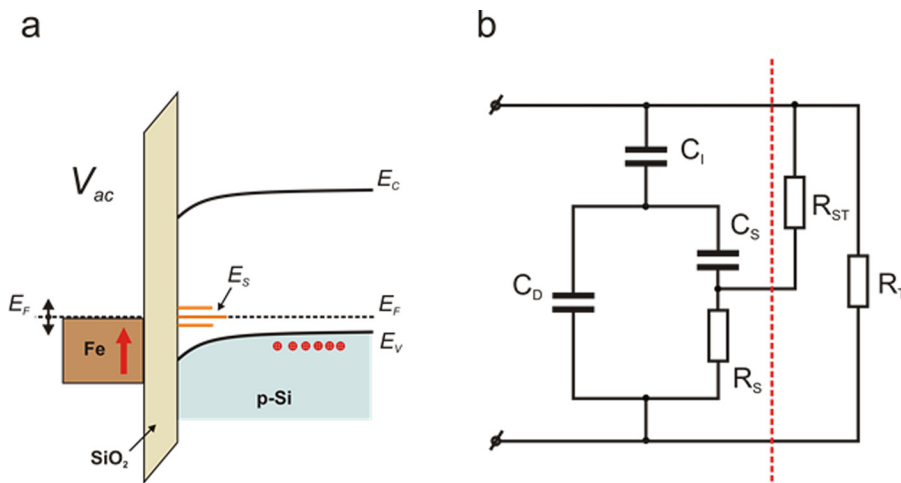


FIG. 2. (a) Schematic band diagram of the Fe/ SiO_2 /p-Si Schottky diode with interface levels (E_s). Ac voltage V_{ac} applied to MIS-transition causes the oscillation of Fermi level E_F in the Fe electrode and, as a result, sweeping of the Fermi level in p-Si through the interface energy levels. (b) Approximate equivalent circuit of the Fe/ SiO_2 /p-Si Schottky diode. C_D and C_I are equivalent capacitances of the semiconductor and insulator layers, respectively; C_S and R_S are equivalent capacitance and resistance, respectively, corresponding to recharging of the interface centers; R_T and R_{ST} are equivalent resistances corresponding to tunneling of electrons to the valence band and on the interface levels, respectively. Dashed line separates the equivalent circuit of the ideal MIS structure (without tunneling).

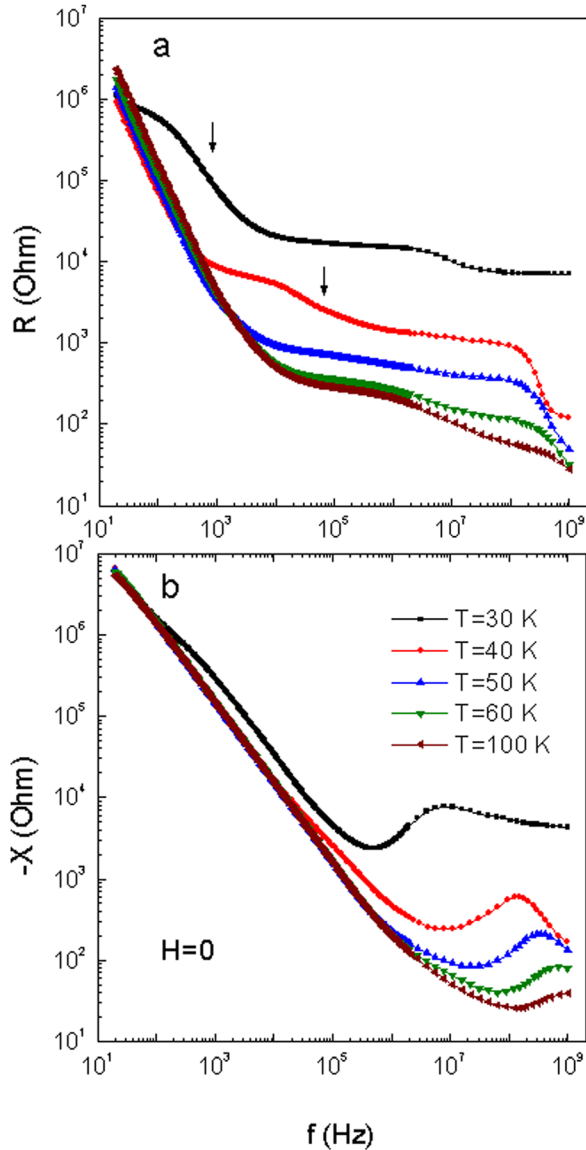


FIG. 3. Frequency dependences of (a) the real and (b) imaginary parts of the impedance at different temperatures for the back-to-back Fe/SiO₂/p-Si diode in zero magnetic field.

especially pronounced in the frequency range 10^7 – 10^8 Hz for all temperatures. As the temperature is decreased, the feature expectedly shifts towards lower frequencies. The step and peak heights are maximum at 40–60 K and decrease beyond this range. The second feature (marked with arrows in the figure) is observed at lower frequencies. It is less pronounced and clearly seen only below 50 K.

The monotonic decrease of R and X with increasing frequency in the low-frequency region is reflected by the fact that on the SiO₂/p-Si interface, an inversion layer forms in which differential capacitance C_D exceeds by far the capacitance of SiO₂ ($C_D \gg C_I$).¹³ At a certain value of the surface potential, the inversion layer appears due to thermal generation of electron-hole pairs in the spatial charge region. As the surface potential is decreased, the density of electrons in the inversion layer decreases due to recombination with holes in the spatial charge region. A decrease in C_D with increasing frequency is caused by a low rate of the

generation-recombination processes. Only at low (5–100 Hz) frequencies where concentration of minority carriers changes with the measuring signal, the capacitance is large. As the frequency is increased, the density of electrons starts lagging the variation in the measuring signal, C_D and, correspondingly, R and X drop.

Two other features are related to recharging of the surface centers. Here, there might be two physical processes responsible for these features. The first one may be related to the presence of two centers with different time constants ($\langle \tau_i \rangle$) that characterize the recharging process. The second possibility is the presence of one type of the center whose recharging is determined by two different mechanisms and, consequently, characterized by two time constants. For example, it can be capture-emission of holes that connects the interface levels and the valence band and is characterized by time ($\langle \tau_B \rangle$). Another possible mechanism is the electron tunneling between the metal and the interface levels through the potential barrier with characteristic time ($\langle \tau_T \rangle$).

B. Impedance in magnetic field

The aim of this study was to investigate the effect of magnetic field on the transport properties of the hybrid Fe/SiO₂/p-Si structure by measuring the ac current. We should emphasize that the special features in behavior of MR and MX seen in varying temperature, frequency, and magnetic field allow us to exclude the mechanisms related to the effect of the magnetoimpedance in ferromagnetic metals, which are solely due to the processes of the ferromagnets magnetization. Furthermore, our estimates indicate that the skin-depth for pure iron at the highest frequency involved is $l_{skin}^{Fe} (1GGz) \approx 125$ nm. We believe it is improbable that for the 5 nm thick Fe-layer, one could observe a strong frequency dependence of the magnetoresistance. Therefore, we can separate the observed effect from magnetoimpedance phenomena in soft ferromagnets¹⁶ and microwave magnetoimpedance.¹⁷ It appeared that the significant value of magnetoimpedance (we actually followed separately the magnetoresistance $MR = 100\% \times (R(H) - R(0))/R(0)$ and magnetoreactance $MX = 100\% \times (X(H) - X(0))/X(0)$) is observed in the temperature range 30–100 K and strongly depends on frequency. Figure 4 shows temperature dependences of MR and MX in a magnetic field of 10 kOe for two different frequencies in the low- and high-frequency regions (1 kHz and 63 MHz).

When measuring the $MR(T)$ dependence at low-frequency ac signal, the effect of magnetic field is strong in the narrow temperature range 30–50 K and insignificant portion of negative magnetoresistance is changed for the narrow intense peak that corresponds to the positive magnetoresistance. Recall that in this range, the characteristic (magneto-sensitive) peak P_m is observed in the $R(T)$ dependence and the corresponding step is observed in the $X(T)$ dependence. In magnetic field, the P_m peak becomes more intense and shifts towards higher temperatures (Fig. 5). This explains the behavior of $MR(T)$, specifically the presence of the portions of negative and positive magnetoresistance. The step in the $X(T)$ dependence in a magnetic field shifts to the

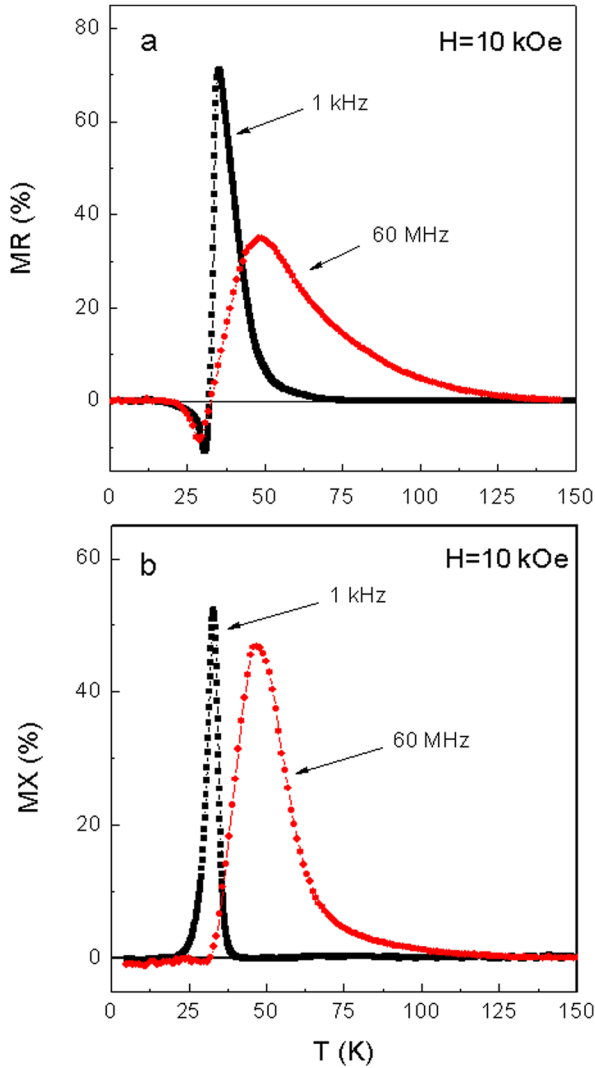


FIG. 4. Temperature dependences of (a) magnetoresistance and (b) magnetoreactance at frequencies of 1 kHz and 60 MHz for the back-to-back Fe/SiO₂/p-Si diode device in a magnetic field of 10 kOe.

high-temperature region (inset in Fig. 5), which causes the narrow intense peak in the $MX(T)$ dependence. By increasing frequency, P_m in the $R(T)$ dependence shifts towards higher temperatures, its intensity rapidly drops, but the relative change in R in a magnetic field remains large. The same scenario is implemented for the imaginary part of the impedance: with increasing frequency, the absolute value of X decreases, but the relative change in reactance MX in a magnetic field in the step area remains large.

Now, referring to the $MR(T)$ and $MX(T)$ dependences obtained at a high (63 MHz) frequency of the measuring signal, we can see that the character of the dependences is the same as in the case of low frequencies (Fig. 4). However, the temperature range in which the effect of magnetic field is strong broadens towards higher temperatures. The maxima in the $MR(T)$ and $MX(T)$ dependences also shift towards higher temperatures and their values decrease. Everything points out that the variation in a magnetic field at different frequencies is related to the same peak P_m in the $R(T)$ dependence corresponding to the step in the $X(T)$ dependence and transforming with frequency variation. In other words,

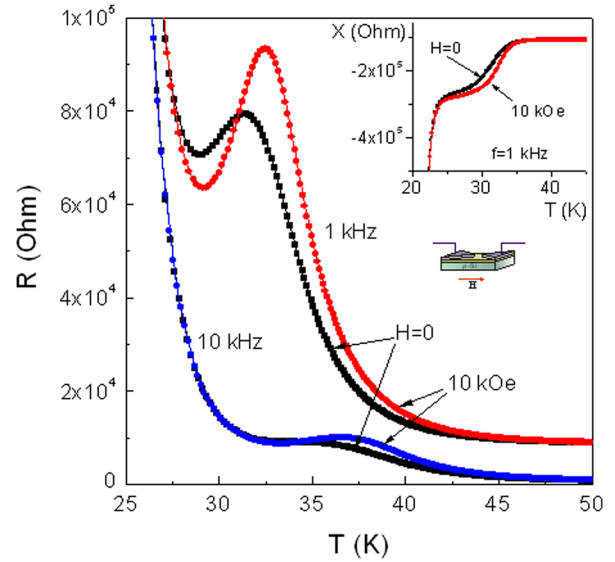


FIG. 5. Behavior of the “magnetosensitive peak” P_m in $R(T)$ (see Fig. 1) in varying magnetic field. Main panel: temperature dependences of the real part of the impedance (R) at frequencies of 1 and 10 kHz in zero magnetic field and in a field of 10 kOe. The inset shows the corresponding behavior of the imaginary part of the impedance (X).

sensitivity to magnetic field is associated with the only type of the surface center. Unfortunately, it is impossible to follow the behavior of P_m in the $R(T)$ dependences at all frequencies, since, as we have already mentioned, this is obscured by the higher intensity peak located at lower temperature (Fig. 1) that corresponds to the other type of the surface center. Although the step in the $X(T)$ dependences is clearly observed up to frequencies above 10 MHz, it is also absorbed by the more intense step coming from the low-temperature side. Nevertheless, the absence of any additional features in the $R(T)$ and $X(T)$ dependences and insensitivity of the intense low-temperature peak (step) to a magnetic field make us believe we observe the only type of the surface center that determines the effect of a magnetic field. We should not exclude, however, that during recharging of this center, the mechanism involving the second, magnetic-field-insensitive type of the center can be implemented. The fact that the peaks overlap suggests possible correlation between the surface centers via charge transport with a certain characteristic time.

Figures 6(a) and 6(b) illustrate the response of the real (R) and imaginary (X) parts of the impedance to the external magnetic field as a function of the measuring signal frequency. It can be seen that the maximum changes in R and X in magnetic field correspond to the Debye features in the $R(f)$ and $X(f)$ dependences (Fig. 3). In the low-temperature region, MR and MX are maximum at 10^2 – 10^3 Hz. As the temperature is increased, the maxima shift to the high-frequency region and lose their intensity. Simultaneously, the peaks in the $MR(f)$ and $MX(f)$ dependences in the high-frequency range 10^7 – 10^9 Hz grow and become the most intense at the temperature of 50 K. With further increase in temperature, these peaks also rapidly lose their intensity and vanish above 100 K. Again we may conclude that the effect of magnetic field is determined by either two types of the

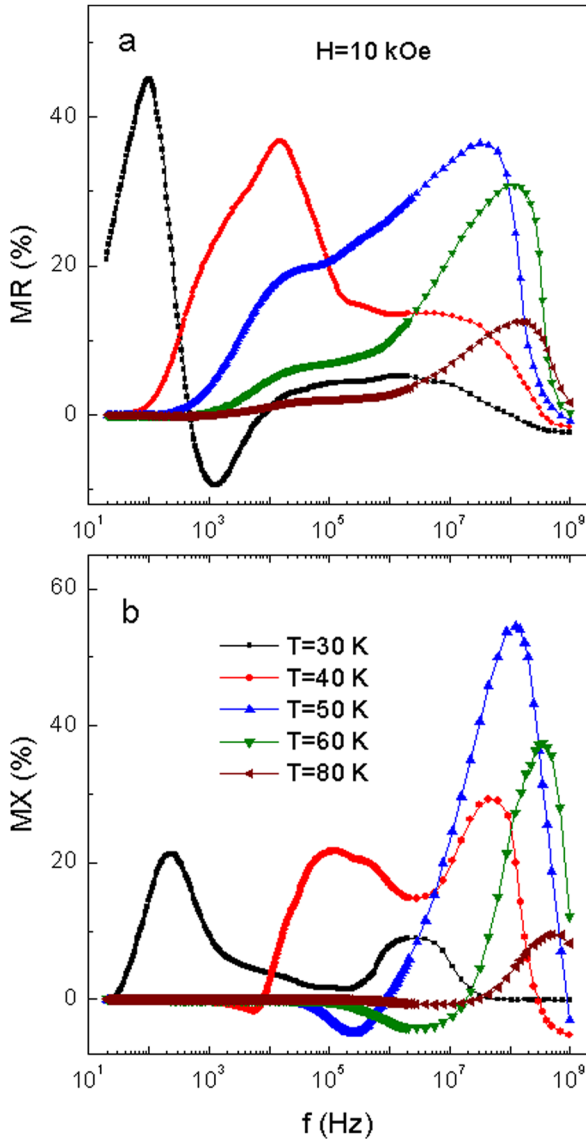


FIG. 6. Frequency dependences of (a) magnetoresistance and (b) magneto-reactance of the back-to-back Fe/SiO₂/p-Si diode device in a magnetic field of 10 kOe at different temperatures.

magneto-sensitive centers or one type of the center that can recharge by different mechanisms with different characteristic times. Taking into account the results of the above analysis, we are inclined to believe in the latter.

C. Possible nature of the magneto-sensitive center

If, as we believe, sensitivity of impedance of the Fe/SiO₂/p-Si structure to magnetic field is determined by one type of the surface center and contribution of different mechanisms to its recharging, the fundamental questions arise: what does this center originate from? Which impurities induce the formation of this center? What is the energy structure of this center?

The analysis of the literature data gives us grounds to suggest that, in our case, the magneto-sensitive center is the iron-ion-bearing one. Indeed, it is known that iron is characterized by enormous complexing activity, i.e., partial or complete ionization and high diffusivity in Si and SiO₂.^{18–20} Iron

is mobile even at room temperature and can rapidly diffuse above 100 °C. Thus, at the technological stage, diffusion of Fe ions through a thin (1.2 nm) SiO₂ layer in the investigated structure is highly probable. This process leads to the formation of impurity charge centers with a Fe ion on the SiO₂/p-Si interface or near it. Either a simple interstitial Fe center or more complex centers can form due to high reactivity of iron. Over 30 such complexes were found and identified in silicon.¹⁸ For p-Si doped with boron, the formation of FeB pairs²¹ is the most probable.

Each center is characterized by its own energy levels in the band gap. An isolated iron ion, which occupies, as a rule, a tetrahedral interstitial site in the silicon lattice acts as a donor (Fe_i^{0/+}) at $E_V + E_D = E_V + 0.4$ eV, where E_V and E_D are the energy of the valence band top and the energy of the center relative to the valence band, respectively. The energy level of (FeB)^{0/+} at $E_V + (0.1 \pm 0.01)$ eV was identified by a few research groups.^{22–24} The donor nature of the FeB pairs was inferred from the resistivity and Hall effect data.²⁵

To determine the energy levels of the magneto-sensitive center in the structure, we analyze the temperature dependences of the real (R) and imaginary (X) parts of the impedance.¹⁴ Under the conditions of thermal equilibrium and zero bias, the $R(T)$ peak and the corresponding $X(T)$ step are observed at temperature T_p at which the charge state of the center changes. Plotting $\omega/T_p^{3/2}$ ($\omega = 2\pi f$) versus $1/T_p$ has to yield the straight line with a slope corresponding to energy E_D of the center with respect to the valence band.

We extracted the value of T_p for frequencies of 1 kHz and 11 MHz in zero magnetic field and at 10 kOe. For convenience, T_p was extracted as the position of inflection point in the $X(T)$ curves; certainly, here we speak about the feature (step) that corresponds to the “magneto-sensitive” peak P_m in the $R(T)$ dependence (Fig. 5). The dependences of $\omega/T_p^{3/2}$ on the reciprocal peak temperature are presented in Fig. 7. Surprisingly, the dependences are not linear in the entire frequency range. Two linear portions can be convincingly

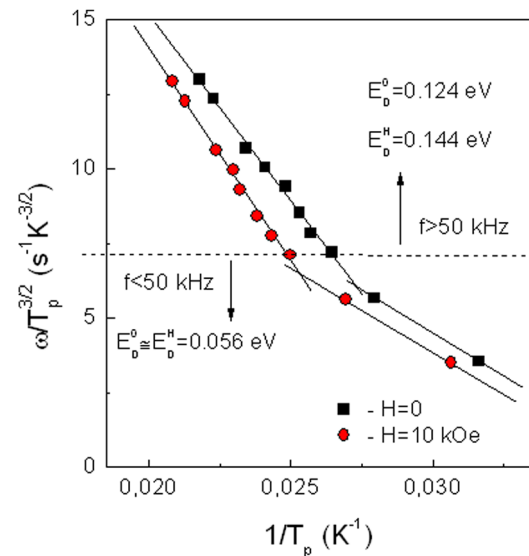


FIG. 7. $\omega/T_p^{3/2}$ versus reciprocal peak temperature $1/T_p$ at 0 and 10 kOe. Straight lines are linear fitting of the portions at frequencies ($\omega/2\pi$) below and above 50 kHz.

distinguished: below and above 50 kHz. In zero magnetic field, we obtain $E_D^0 = 0.056$ eV in the low-frequency region and 0.124 eV at $f > 50$ kHz. Thus, we may assume the existence of two surface centers with different energy states in the band gap. Still, as before, we are inclined to believe that there is only one center present here but different recharging mechanisms take place.

In the latter case, the approach used by us to determine E_D is not always valid. Indeed, it is based on the assumption that only generation-recombination processes occur that connect the impurity centers and the states in the valence band and these processes have the same relaxation times. However, we have already mentioned that for the thin SiO₂ layer, we cannot exclude tunneling of electrons through the potential barrier between the impurity centers near the SiO₂/p-Si interface and the Fe electrode. Delay of the impurities recharging with regard to the tunneling of electrons is believed to be due to different relaxation times.

The value $E_D^0 = 0.124$ eV obtained by us from the data for $f > 50$ kHz that fit the straight line with good accuracy is very close to the energy of the donor center (FeB)^{0/+}. This gives us grounds to assume the formation of such centers and the fact that in the high-frequency region, the relaxation time of the centers is determined by recharging processes occurring mainly with the participation of the valence band of the semiconductor: emission of holes in the valence band and capture of free holes (in other words, the dependence of $\omega/T_p^{3/2}$ on $1/T_p$ should be linear). In the low-frequency region, relaxation with regard to the tunneling of electrons is added. Here, the position of the T_p peak in the real part of the impedance depends differently on frequency, i.e., the analysis used for obtaining E_D may not be reliable.

Figure 8 presents schematic energy structure of the MIS transition and two possible mechanisms of recharging for the interface centers. As was mentioned, it is believed that first recharging of the centers with the participation of the valence band occurs and then the tunneling mechanism is triggered when the Fermi level, driven by the variation in the voltage across the MIS structure, sweeps through the interface energy levels.

Note one more point that may point to the fact that only one type of the center is responsible for the sensitivity of the impedance to a magnetic field. In Figure 7, the sharp change in the behavior of the dependences near 50 kHz is observed.

At the same time, no features in the behavior of the peak in the $R(T)$ and the step in the $X(T)$ near this frequency are observed (Fig. 1). By looking at the behavior of the step in the $X(T)$ dependences obtained at different frequencies, we can see that this is the same feature, i.e., the feature determined by the same type of the interface state.

D. Mechanism of the effect of magnetic field

So what could be the mechanism of the effect of a magnetic field on the real and imaginary parts of the impedance? As was mentioned in Introduction, we failed to find any literature data on the transport properties of the MIS transition on an alternating current under the action of a magnetic field. A few works available^{20,26–28} were devoted to magnetoresistive effects on a direct current and the mechanisms suggested by the authors were related, as a rule, to the processes occurring in the semiconductors bulk. First of all, this is magnetoresistance originated from scattering by magnetic impurities or impurities with the spin-orbit coupling, shrinkage of the impurity wave functions in magnetic field, and various mechanisms of weak localization caused by spin splitting and orbital effects.²⁹ These mechanisms are implemented with participation of the carriers moving in the volume of semiconductor, so they are hardly applicable to our situation.

In our case, as we stated above, the features of the transport properties on an alternating current are determined by recharging the surface centers of the SiO₂/p-Si interface. We should apparently search for the source of the magnetotransport influence on the ac current in the magnetic-field resolved reconstruction of the energy structure of the interface centers. The direct evidence for this is demonstrated, in particular, in Fig. 5, where the “magnosensitive peak” P_m in the $R(T)$ dependence in a magnetic field shifts and shrinks. Recall that the position of the peak is determined actually by the average relaxation time $\langle\tau_i\rangle$ and its width, by the relaxation time distribution function. Taking into account $\tau_i = \tau_0 \exp(E_i/k_B T)$, the position and shape of the peak reflect the energy distribution of the density of the interface levels. Thus, the magnetic field gradually narrows the level-density distribution of the “magnetic” impurity centers and shifts it towards higher energies relative to the valence band. Analysis of the dependences in Fig. 7 shows that magnetic field of 10 kOe leads to the shift of the energy levels by at

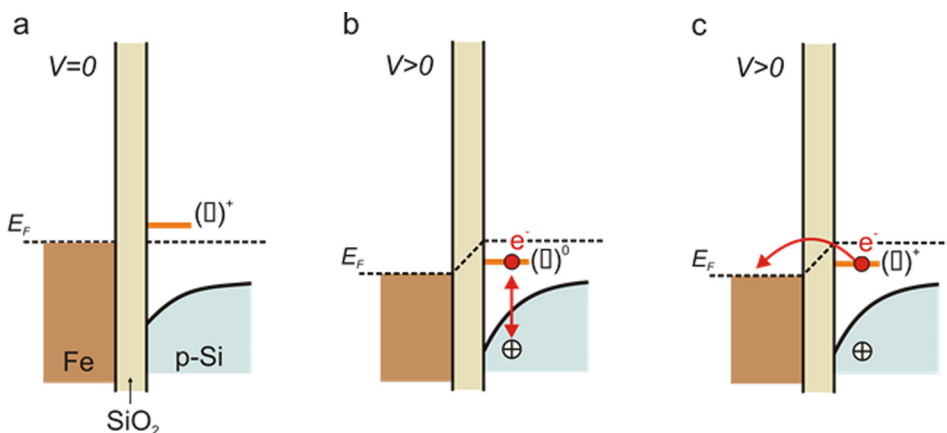


FIG. 8. (a) Schematic band diagram of the Fe/SiO₂/p-Si Schottky diode with a donor surface center (\square)^{0/+}. (b) Recharging of the centers at varying voltage by thermal generation of holes to the valence band (fast process). (c) Recharging by tunneling of electrons from the surface levels into the Fe electrode (slow process).

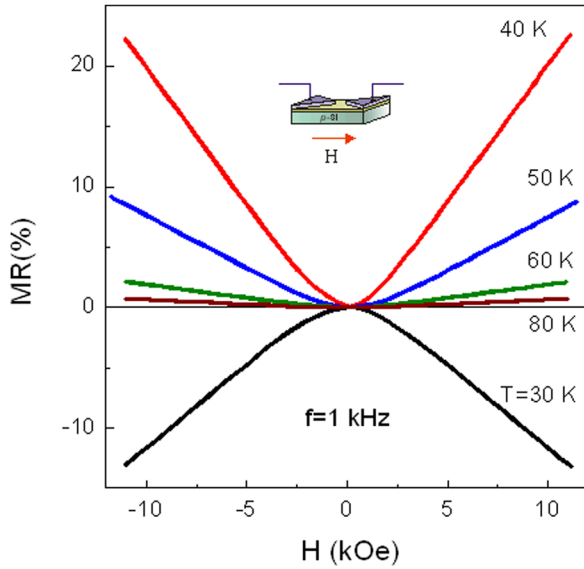


FIG. 9. Magnetoresistance MR as a function of a magnetic field at different temperatures for the back-to-back $\text{Fe}/\text{SiO}_2/\text{p-Si}$ diode device. The ac voltage frequency is 1 kHz.

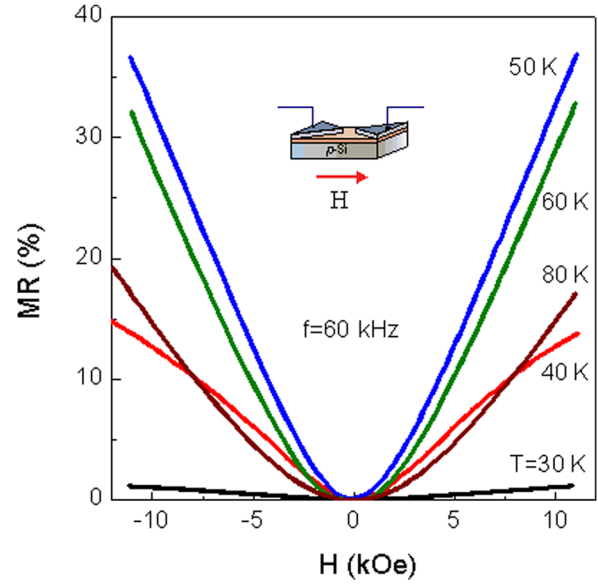


FIG. 10. Magnetoresistance MR as a function of a magnetic field at different temperatures for the back-to-back $\text{Fe}/\text{SiO}_2/\text{p-Si}$ diode device. The ac voltage frequency is 60 MHz.

least 20 meV. Generally, the shift of the energy levels of the impurity centers in magnetic field towards higher energies is typical to doped semiconductors. This effect was observed, for example, in p-doped Si (Ref. 26) and n^- -type GaAs.²⁷ Two possible models were discussed: (1) shrinkage of the impurity center wave functions caused by magnetic field; (2) splitting of the impurity band into lower and higher subbands. However, in neither case, specific microscopic mechanisms of the change in the electronic structure of the impurity centers in a magnetic field were clarified. Simple estimations show that the Zeeman splitting of the levels ($\Delta E_Z = g\mu_B HS$, where $g = 2$ and $S = 3/2$ for the $(\text{FeB})^{0/+}$ center discussed above) can yield, at best, ~ 0.1 meV at 10 kOe, which in no way can explain the experimentally observed shift of the impurity electron levels.

The magnetic-field dependences of MR and MX obtained by us at different temperatures also do not explain the effect of magnetic field on the ac transport properties of the $\text{Fe}/\text{SiO}_2/\text{p-Si}$ structure. At low frequencies in weak (up to ~ 2 kOe) magnetic fields, the $MR(H)$ dependence is parabolic; in strong magnetic fields, the dependence becomes linear with good accuracy (Fig. 9). This is observed for all temperatures. In the high-frequency region, the field dependence of the magnetoresistance is different at different temperatures (Fig. 10). At $T = 30$ K, the $MR(H)$ dependence is similar to the low-frequency one. At $T = 40$ K, the $MR(H)$ dependence is more complex: the parabolic portion at $H < 5$ kOe and the $H^{1/2}$ -type dependence at $H > 5$ kOe. At higher temperatures ($T \geq 50$ K), the $MR(H)$ dependences become parabolic over the entire field range. Concerning magneto-reactance, the $MX(H)$ dependences in all the cases are similar to $MR(H)$, so we do not show them. Difference in the behavior of $MR(H)$ at low and high frequencies again gives us grounds to state that the high- and low-frequency features in the behavior of the impedance can be determined by different processes of recharging of the interface centers. More

specific conclusions are difficult to be drawn at this stage. The key question arising in studying hybrid structures is whether the spin-dependent tunneling through a potential barrier somehow contributes to magnetoresistance and magneto-reactance. Note two works whose authors mentioned that the surface states can effectively participate in the spin-polarized transport in hybrid tunnel structures.^{30,31} In both studies, the authors suggested that these states play a role of intermediate states for spin-polarized electrons upon tunneling between a ferromagnetic electrode and a semiconductor volume. In fact, they can act as an accumulation layer for the spin-polarized carrier in which the spin lifetime is large. This is interesting for spintronic application, for example, enhancing spin injection from a ferromagnet into a semiconductor.

In our case, unlike the proposed mechanism, tunneling can occur only between the ferromagnetic electrode (Fe) and the localized interface centers through the SiO_2 layer; the semiconductor body is not involved in the ac transport. Obviously, the spin-dependent tunneling should manifest itself mainly within the field range where the ferromagnetic electrode is magnetized, i.e., from -2 to $+2$ kOe (Fig. 11). In addition, the contribution of the magnetoresistive effect determined by the spin-dependent tunneling has to be negative (negative magnetoresistance). Above we suggested that the contribution of the tunneling processes to recharging of the impurity centers can be expected in the low-frequency region at low temperatures. It is indicative that in the frequency dependence of MR obtained at different temperatures, there is merely a small portion of negative magnetoresistance at $T = 30$ K (Fig. 6). At this stage of the investigation, it is difficult to answer the question about the contribution of the spin-dependent tunneling to magnetoimpedance, but some results obtained suggest implementation of such a mechanism. It appeared that if the ferromagnetic electrode (Fe) is completely demagnetized and the structure

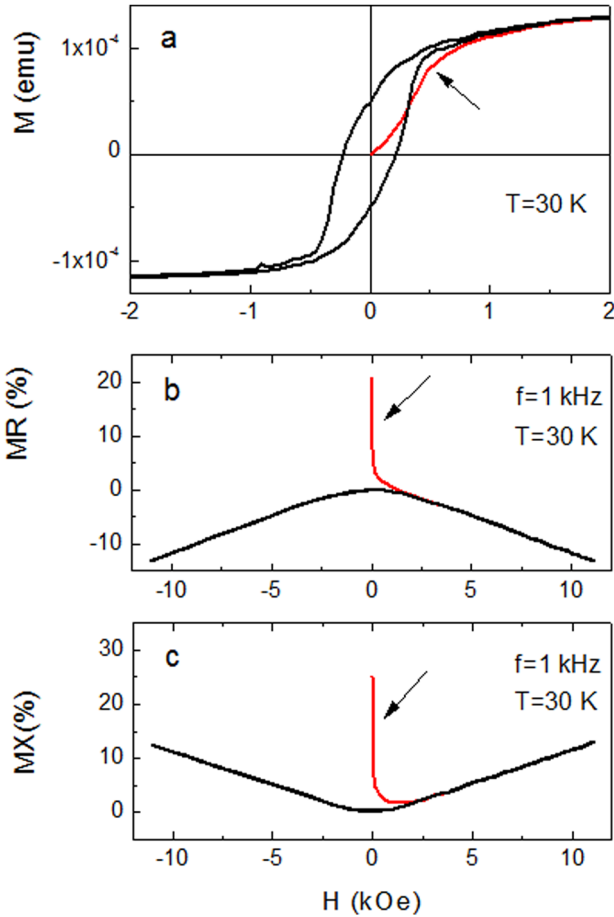


FIG. 11. Magnetization (a) of the Fe/SiO₂/p-Si structure, M , as a function of magnetic field at 30 K. (b) Magnetoresistance (b) and magnetoreactance (c) and as functions of the magnetic field at 30 K for frequency of the ac voltage 1 kHz. The arrows indicate the portions of the dependencies recorded during a first scanning of a magnetic field after zero-field cooling of the structure.

to be measured is cooled at low temperatures in zero magnetic field, then in the $MR(H)$ and $MX(H)$ dependences, a portion of negative magnetoresistance at 0–2 kOe is observed (Fig. 11(b)), which is similar to the primary curve of magnetization of the Fe layer (Fig. 11(a)). We should emphasize that magnetization M of the Fe layer saturates just in fields of about 1.5 kOe. At the next passages of the field from -10 to $+10$ kOe, the mentioned feature in $MR(H)$ is not observed and in the range from -2 to $+2$ kOe, the $MR(H)$ dependence appears to be smooth and parabolic. The magnetization reversal curve $M(H)$ for the Fe layer acquires the typical hysteretic form. Saturation of the $M(H)$ dependence (at ~ 2 kOe) corresponds to the transition of $MR(H)$ from the parabolic dependence to the linear one. The correlation between $MR(H)$ and $M(H)$ suggests there is strong coupling of the impurity magnetic state in the ferromagnetic layer to the ac magnetotransport properties of the Fe/SiO₂/p-Si structure. This, in turn, suggests the presence of the spin-dependent tunneling of carriers through the potential barrier between the Fe electrode and the magnetic centers located near the SiO₂/p-Si interface.

Note that with increasing frequency of the alternating current, the weak-field feature in $MX(H)$ rapidly vanishes and is practically absent above 50 kHz. We should recall that

it is this frequency that was obtained in the analysis of the dependences in Fig. 7 and below which, in our opinion, tunnel recharging of the interface centers switches on. This feature is rapidly suppressed and disappears completely together with the effect of the magnetic field on the low-frequency ac transport at temperatures above 50 K.

IV. CONCLUSIONS

Having investigated the ac transport in the Fe/SiO₂/p-Si structure with the Schottky barrier in a magnetic field, we demonstrated that the structure exhibits considerable magnetoimpedance, which exceeds by far the dc magnetoresistance. The effect of the magnetic field on the impedance is pronounced only in the specified ranges of temperatures and excitation frequencies. Attempted systematic study of the real and imaginary parts of the impedance leads us to conclude that the features of the ac transport properties are caused by recharging of the surface centers at the SiO₂/p-Si interface. Recharging is implemented via either capture-emission of the carriers that connect the interface levels and the valence band or electron tunneling through the potential barrier between the metal electrode and the interface levels. Most likely, the magnetic-field-sensitive center is a donor-like center that contains Fe and B ions (FeB)^{0/+}. The B ion enters p-Si as a dopant; Fe diffuses through the thin SiO₂ layer. Sensitivity of the impedance to magnetic field is caused by reconstruction of the energy structure of magnetic centers in the field, which, in turn, affects recharging of the centers. At this stage of the study, we cannot determine the microscopic mechanism of sensitivity of the transport properties of the structure to magnetic field. However, we can already state that the spin-dependent tunneling of electrons between the ferromagnetic electrode and the surface levels on the interface between the dielectric and semiconductor in the Fe/SiO₂/p-Si structure contributes to magnetoimpedance.

The results obtained are the first observation of the giant magnetoresistive effect in hybrid structures in the alternating current. As a matter of fact, these results open a novel direction in silicon spintronics: the use of the spin-dependent tunneling and spin transport as a whole in hybrid structures with the participation of “magnetic” surface centers. Now, taking into account the high level achieved in the development of modern semiconductor technology, direct fabrication of the “magnetic” surface centers with specified properties in hybrid structures can be planned, which would give an opportunity of implementing the magneto-dependent effects for spintronic applications at room temperature in specified frequency ranges.

ACKNOWLEDGMENTS

This study was supported by the Russian Foundation for Basic Research, Project No. 11-02-00367-a; the Presidium of the Russian Academy of Sciences, program Quantum Mesoscopic and Disordered Structures, Project No. 20.8; the Division of Physical Sciences of the Russian Academy of Sciences, program Spin Phenomena in Solids Nanostructures and Spintronics, Project No. II.4.3; the Siberian Branch of

the Russian Academy of Sciences, Integration Projects Nos. 85 and 102, and the Federal target program Scientific and Pedagogical Personnel of Innovative Russia (State Contract No. NK-556P_15).

- ¹A. Fert, *Thin Solid Films* **2–5**, 517 (2008).
- ²S. P. Dash, S. Sharma, R. S. Patel, M. P. de Jong, and R. Jansen, *Nature (London)* **462**, 491 (2009).
- ³I. Appelbaum, B. Huang, and D. J. Monsma, *Nature (London)* **447**, 295 (2007).
- ⁴V. V. Osipov and A. M. Bratkovsky, *Phys. Rev. B* **72**, 115332 (2005).
- ⁵I. Zutic, J. Fabian, and S. D. Sarma, *Rev. Mod. Phys.* **76**, 323 (2004).
- ⁶H. Kaiju, S. Fujita, T. Morozumi, and K. Shiiki, *J. Appl. Phys.* **91**, 7430 (2002).
- ⁷T. Y. Peng, S. Y. Chen, L. C. Hsieh, C. K. Lo, Y. W. Huang, W. C. Chien, and Y. D. Yao, *J. Appl. Phys.* **99**, 08H710 (2006).
- ⁸S. K. Barik and R. Mahendiran, *J. Appl. Phys.* **109**, 07D724 (2011).
- ⁹W. C. Chien, C. K. Lo, L. C. Hsieh, Y. D. Yao, X. F. Han, Z. M. Zeng, T. Y. Peng, and P. Lin, *Appl. Phys. Lett.* **89**, 202515 (2006).
- ¹⁰P. Padhan, P. LeClair, A. Gupta, K. Tsunekawa, and D. D. Djayaprawira, *Appl. Phys. Lett.* **90**, 142105 (2007).
- ¹¹M.-F. Kuo, C.-M. Fu, X.-F. Han, C.-O. Chang, and C.-S. Chou, *J. Appl. Phys.* **109**, 07C718 (2011).
- ¹²R. Jansen, B.-C. Min, and S. P. Dash, *Nature Mater.* **9**, 133 (2009).
- ¹³N. V. Volkov, A. S. Tarasov, E. V. Eremin, S. N. Varnakov, S. G. Ovchinnikov, and S. M. Zharkov, *J. Appl. Phys.* **109**, 123924 (2011).
- ¹⁴D. L. Losee, *J. Appl. Phys.* **46**, 2204 (1975).
- ¹⁵S. M. Sze, *Semiconductor Devices* (Wiley, New York, 1985).
- ¹⁶S. E. Lofland, S. M. Bhagat, S. D. Tyagi, Y. M. Mukovskii, S. G. Karabashchev, and A. M. Balbashov, *J. Appl. Phys.* **80**, 3592 (1996).
- ¹⁷J. M. Barandiaran, A. G. Arribas, J. L. Munoz, and G. V. Kurlyandskaya, *IEEE Trans. Magn.* **38**, 3051 (2002).
- ¹⁸A. A. Istratov, H. Hieslmair, and E. R. Weber, *Appl. Phys. A* **69**, 13 (1999).
- ¹⁹M. Kanoun, R. Benabderrahmane, C. Duluard, C. Baraduc, N. Bruyant, A. Bsiesy, and H. Achard, *Appl. Phys. Lett.* **90**, 192508 (2007).
- ²⁰S. Witanachchi, H. A. Mourad, H. Srikanth, and P. Mukherjee, *Appl. Phys. Lett.* **90**, 052102 (2007).
- ²¹H. Nakashima, T. Sadoh, and T. Tsurushima, *Phys. Rev. B* **49**, 16983 (1994).
- ²²K. Wunstel and P. Wagner, *Appl. Phys. A* **27**, 207 (1982).
- ²³H. Lemke, *Phys. Status Solidi A* **64**, 215 (1981).
- ²⁴S. D. Brotherton, P. Bradley, and A. Gill, *J. Appl. Phys.* **57**, 1941 (1985).
- ²⁵K. Graff and H. Pieper, *J. Electrochem. Soc.* **128**, 669 (1981).
- ²⁶J. J. H. M. Schoonus, F. L. Bloom, W. Wagemans, H. J. M. Swagten, and B. Koopmans, *Phys. Rev. Lett.* **100**, 127202 (2008).
- ²⁷T. W. Hickmott, *Phys. Rev. B* **46**, 12324 (1992).
- ²⁸Z. G. Sun, M. Mizuguchi, T. Manago, and H. Akinaga, *Appl. Phys. Lett.* **85**, 5643 (2004).
- ²⁹P. A. Lee and T. V. Ramakrishnan, *Rev. Mod. Phys.* **57**, 297 (1985).
- ³⁰M. Tran, H. Jaffres, C. Deranlot, J.-M. George, A. Fert, A. Miard, and A. Lemaitre, *Phys. Rev. Lett.* **102**, 036601 (2009).
- ³¹R. Jansen, A. M. Deac, H. Saito, and S. Yuasa, *Phys. Rev. B* **85**, 134420 (2012).